Zircon lutetium–hafnium isotope map of Western Australia

Y Lu, MTD Wingate, AIS Kemp[1], RH Smithies, K Gessner, SP Johnson, SS Romano, DR Mole[2], CL Kirkland[3] and EA Belousova[4,5]

1 School of Earth Sciences, The University of Western Australia, Crawley, WA 6009, Australia
2 Geoscience Australia, GPO Box 378, Canberra, ACT 2601, Australia
3 Timescales of Mineral Systems Group, School of Earth and Planetary Sciences, Curtin University, Perth, WA 6102, Australia
4 ARC Centre of Excellence for Core to Crust Fluid Systems (CCFS) and GEMOC, Macquarie University, New South Wales 2109, Australia
5 Department of Resources, Geological Survey of Queensland, Brisbane, Australia

Abstract

Zircon lutetium–hafnium (Lu–Hf) isotope maps are used to characterize lithospheric architecture through time, to help understand crustal evolution and mineral system distributions, and play an increasingly important role in mineral exploration (Mole et al., 2014, 2019, 2021; Hou et al., 2015; Wang et al., 2016; Lu et al., 2022b). Here we present a revised Lu–Hf isotope map of Western Australia that updates previously released data (Lu et al., 2021) with 1311 new analyses from 55 samples, for a total of 14 059 analyses from 778 samples (Figs 1, 2).

These isotope maps (Fig. 2) are based on Lu–Hf data for dated magmatic zircons from felsic igneous rocks, which provide a window into the age and compositional variation of the middle and lower continental crust where most felsic magmas are generated (Champion and Huston, 2016). Lu–Hf isotope data for zircons from mafic igneous, sedimentary, and metamorphic rocks, and for xenocrystic zircons, were not used in constructing the isotope maps. However, their sample-level information is included as a separate layer. Spot-level data for all samples are provided as a CSV file.

Initial $^{176}Hf/^{177}Hf$ and ε_{Hf} values of all zircons were calculated using the ^{176}Lu decay constant (1.867×10^{-11} a^{-1}) of Söderlund et al. (2004) and the CHUR (CHondritic Uniform Reservoir) value [$^{176}Lu/^{177}Hf$ (present day) = 0.0336 and $^{176}Hf/^{177}Hf$ (present day) = 0.282785] of Bouvier et al. (2008). For each analysis, a two-stage depleted mantle model age (T_{DM}^2) is calculated, which assumes that the parental magma of the zircon was produced from a volume of average continental crust extracted from depleted mantle. T_{DM}^2 estimates the average age of the crustal source of the igneous rocks. Parameters used for calculation of T_{DM}^2 include depleted mantle $^{176}Hf/^{177}Hf$ (present day) = 0.283238 and $^{176}Lu/^{177}Hf$ (present day) = 0.03976 (Vervoort et al., 2018), and average continental crust of $^{176}Lu/^{177}Hf$ (present day) = 0.012 (Spencer et al., 2020). Crustal residence time (T_{CR}), the difference between T_{DM}^2 and magmatic crystallization age, is also calculated for each analysis, and provides an estimate of the average length of time the source of the igneous rocks resided in the crust.

Evolution of the Earth's mantle is a topic of debate in geoscience, including whether mantle depletion occurred at 4.56, 4.5 or 3.8 Ga (Griffin et al., 2002; Blichert-Toft and Puchtel, 2010; Kemp et al., 2015; Vervoort and Kemp, 2016; Fisher and Vervoort, 2018). The model chosen affects values calculated for T_{DM}^2 and T_{CR}, particularly for zircons older than 3.8 Ga. Furthermore, the $^{176}Lu/^{177}Hf$ ratio used to model isotopic evolution is an estimate and imparts significant uncertainty to any model age (see Vervoort and Kemp, 2016). Therefore, T_{DM}^2 and T_{CR} are used here mainly for qualitative comparison purposes because gradients in T_{DM}^2 and T_{CR} may be more insightful than their absolute values. Nevertheless, model ages potentially highlight underlying patterns related to crustal composition and structure (Lu et al., 2022b).

The Lu–Hf isotope data have been filtered to exclude data with U–Pb age discordance >10%, $^{176}Yb/^{177}Hf$ >0.2, and ε_{Hf} 1σ uncertainty >1.5 epsilon units (Belousova et al., 2010). The median $\varepsilon_{Hf(i)}$, T_{DM}^2 and T_{CR} are then calculated for each felsic igneous rock. The isotope maps were created from median T_{DM}^2 and T_{CR} values, using the natural neighbour interpolation tool in ArcGIS Spatial Analyst, and are presented as both classified (natural breaks classification, Fig. 2a,c) and stretched

(Histogram Equalize type, Fig. 2b,d) raster datasets. The spatial interpolation of isotope data shown in Figure 2 follows the approach of Champion and Huston (2016), who found that natural neighbour interpolation using natural breaks in data values produced isotope maps more consistent with known geology than other interpolation methods.

The model age (T_{DM}^2) maps highlight the distinction between Archean cratons (T_{DM}^2 >2.6 Ga) and Proterozoic orogens (T_{DM}^2 <2.4 Ga). Granitic samples from basement rocks beneath the Canning Basin show similar T_{DM}^2 to those in the Musgrave, Madura and Coompana Provinces, but are different to those from the North and West Australian Cratons (NAC and WAC). This suggests the existence of a subsurface Proterozoic terrane, the Percival Lakes Province, between the NAC and WAC (Fig. 2a, b; Lu et al., 2022b; Zhao et al., 2022). Strong isotope gradients are typically associated with major crustal boundaries and are potentially important for localizing mineral systems (Fig. 2; Martin et al., 2022).

Some isotope gradients may not be as pronounced in the statewide map as they might be on more detailed maps of individual regions. Users should download the isotope data and create their own contour maps for particular areas to enhance the isotope gradients in those areas. An example is provided for the Archean Yilgarn Craton (Fig. 3), which provides a more detailed image of the architecture of the Kalgoorlie–Kurnalpi region, a world-class Archean gold province (Witt et al., 2020). It shows that the most juvenile domain developed in the southern Kalgoorlie Terrane and the central to northern Kurnalpi Terrane, supporting the existence of northeast-trending basement structures suggested by granite geochemistry (Smithies et al., 2018) and previous interpretations of variable rift architecture along a cryptic Kalgoorlie Shear Zone (Mole et al., 2019).

Insights into crustal evolution can be gained by visualizing the variation with age of median zircon $\varepsilon_{Hf(i)}$, T_{DM}^2 and T_{CR} for both mafic and felsic igneous rocks (Fig. 4). From c. 3600 to 500 Ma, mafic and felsic igneous rocks show overlapping zircon $\varepsilon_{Hf(i)}$, T_{DM}^2 and T_{CR}, suggesting coupled Lu–Hf isotope evolution in mafic and felsic igneous rocks. This is in contrast to the whole-rock Sm–Nd isotope record which indicates mafic and felsic igneous rocks from c. 3730 to 2500 Ma have overlapping $\varepsilon_{Nd(i)}$, T_{DM}^2 and T_{CR}, but since <2500 Ma, mafic rocks generally yield higher $\varepsilon_{Nd(i)}$ and lower T_{DM}^2 and T_{CR} than felsic rocks at a given age (Lu et al., 2022a). The different pattern between the Lu–Hf and Sm–Nd systems suggests that most zircon-crystallizing mafic magmas (e.g. gabbros) have been contaminated by continental crust.

Felsic igneous rocks record sources requiring episodic juvenile mantle input to have occurred at c. 3566, 3440, 3300, 3200, 3000, 2800, 2700, 1800 and 1400 Ma, as well as reworking of existing crust with T_{DM}^2 up to c. 3920 Ma (Fig. 4). Increasing T_{CR} for both mafic and felsic rocks from c. 3600 to 500 Ma is consistent with secular crustal maturation observed in other isotope systems, such as whole-rock Sm–Nd and zircon oxygen isotopes (Fig. 4c; Valley et al., 2005; Lu et al., 2022a,c).

There are few Lu–Hf data (or whole-rock Sm–Nd and zircon oxygen isotope data) for mafic or felsic igneous rocks between 2500 and 2000 Ma (Fig. 4), consistent with the apparent scarcity of rocks of this age in Western Australia (Lu et al., 2022a,c). However, xenocrystic zircons of this age are common and have mainly heavy $\delta^{18}O$ values. This implies that felsic magmatism during this interval involved significant reworking of supracrustal materials, and that those magmatic rocks were mostly emplaced at depth and not exposed at the surface. This is most likely because the early Paleoproterozoic was dominated by orogenic compression, which trapped magmas at deep crustal levels (Loucks, 2021; Lu et al., 2022a).

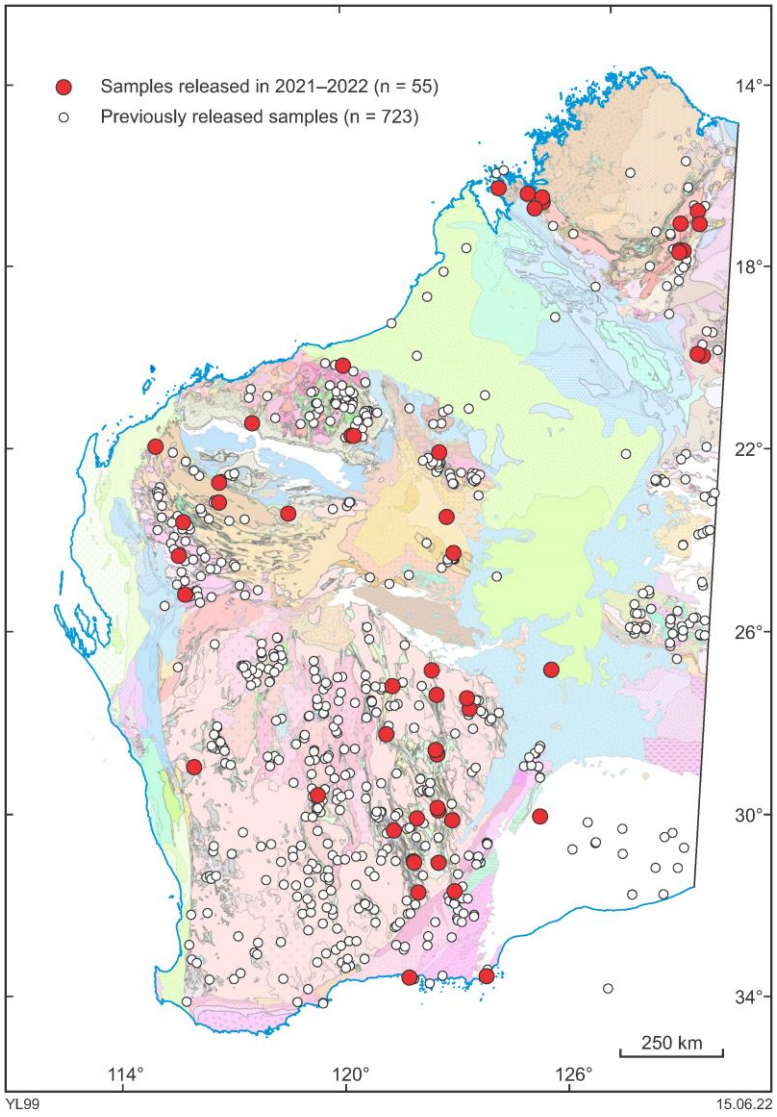

Figure 1. **Locations of new and previously released Lu–Hf isotope samples, shown on the 1:2.5 million interpreted bedrock geology map**

Acquisition of Lu–Hf isotope data by the Geological Survey of Western Australia (GSWA) was funded by the Exploration Incentive Scheme (EIS), and conducted using multi-collector inductively coupled plasma mass spectrometry (MC-ICPMS) in the Centre for Geochemical Evolution and Metallogeny of Continents (GEMOC); the ARC Centre of Excellence for Core to Crust Fluid Systems (CCFS) at Macquarie University; and in the Centre for Microscopy, Characterization and Analysis (CMCA) at The University of Western Australia.

How to access

The data layer is best accessed using GeoVIEW.WA. This online interactive mapping system allows data to be viewed and searched together with other datasets, including GSWA and Geoscience Australia geochronology data, geological maps, and mineral exploration datasets. The Zircon lutetium–hafnium isotope map digital data are also available as a free download from the Data and Software Centre via Datasets — Statewide spatial datasets — Geochronology & Isotope Geology — Zircon lutetium-hafnium isotope map, as ESRI shape files and MapInfo TAB files. All spot-level zircon data are provided as a CSV file. These datasets are subject to ongoing updates as new data are generated.

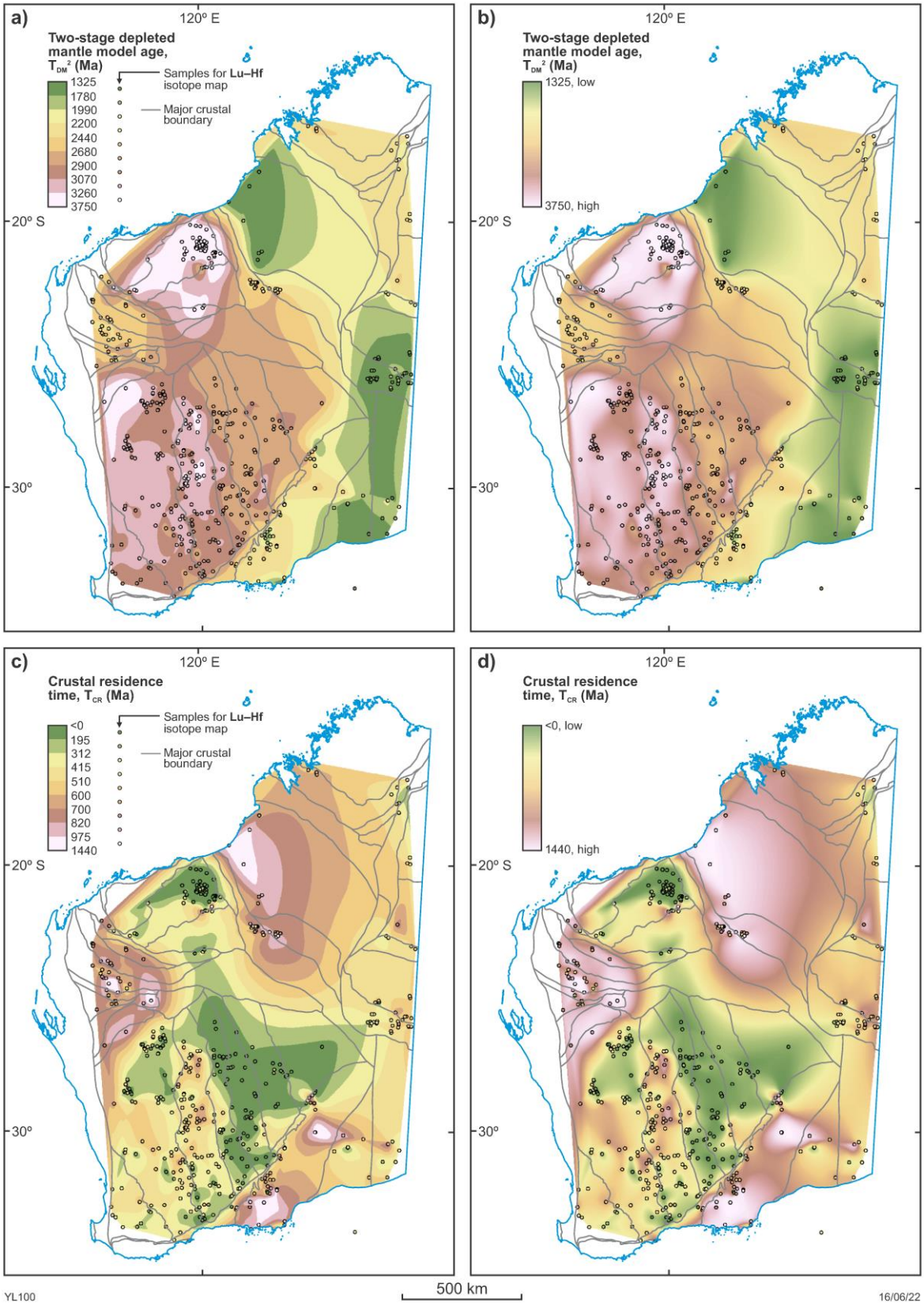

Figure 2. **Lu–Hf isotope maps for zircon samples of felsic igneous rocks in Western Australia. T_{DM}^2 and T_{CR} maps are presented as classified (a and c) and stretched (b and d) raster images interpolated by natural neighbour interpolation. Symbols show the locations of zircon Lu–Hf samples used for isotope mapping. Major crustal boundaries (grey lines) are from Martin et al. (2022)**

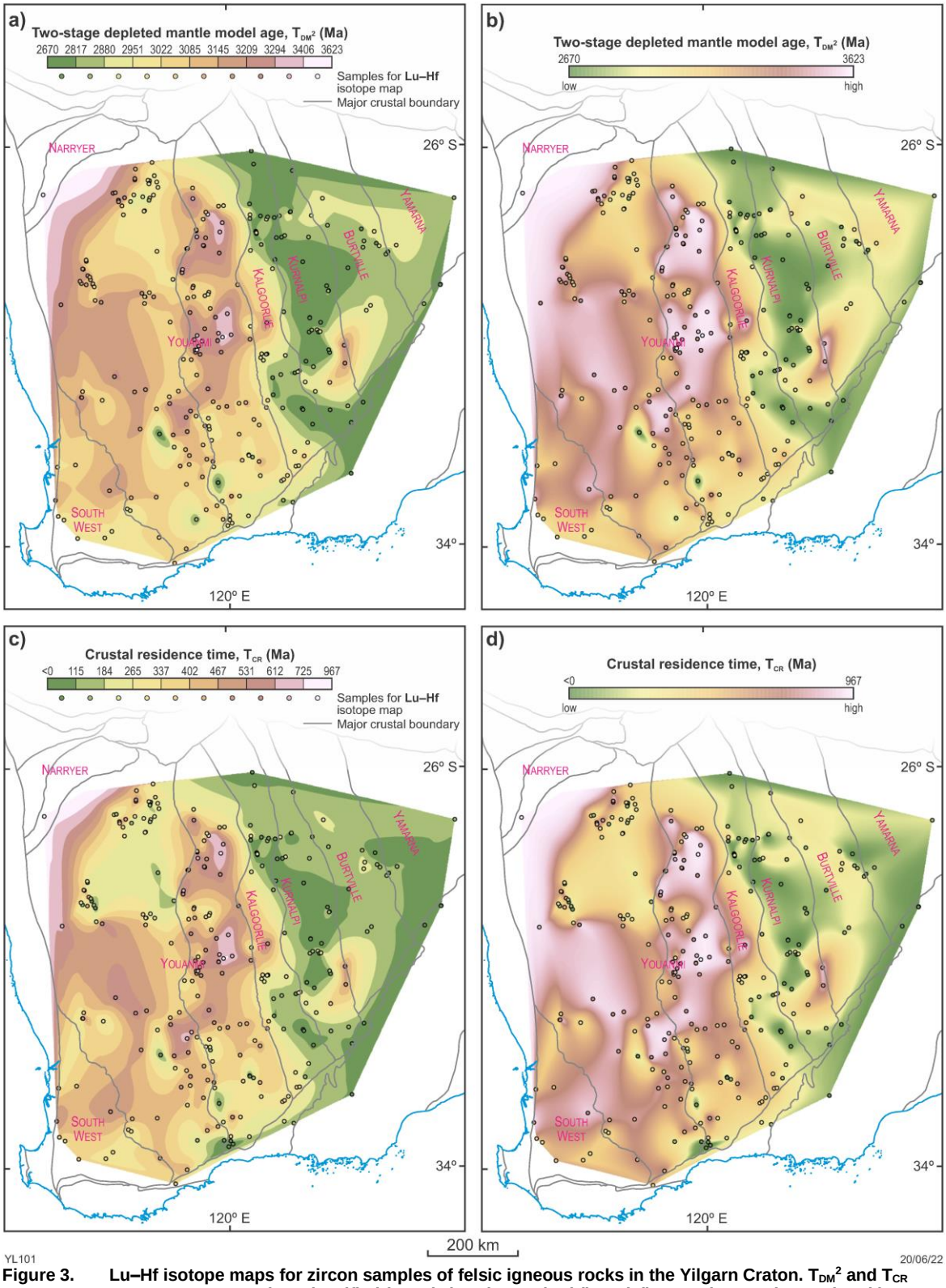

Figure 3. **Lu–Hf isotope maps for zircon samples of felsic igneous rocks in the Yilgarn Craton. T_{DM}^2 and T_{CR} maps are presented as classified (a and c) and stretched (b and d) raster images interpolated by natural neighbour interpolation. Symbols show the locations of zircon Lu–Hf samples used for isotope mapping. Major crustal boundaries (grey lines) are from Martin et al. (2022). Only samples older than 2600 Ma are used here to reveal the Archean crustal architecture of the craton**

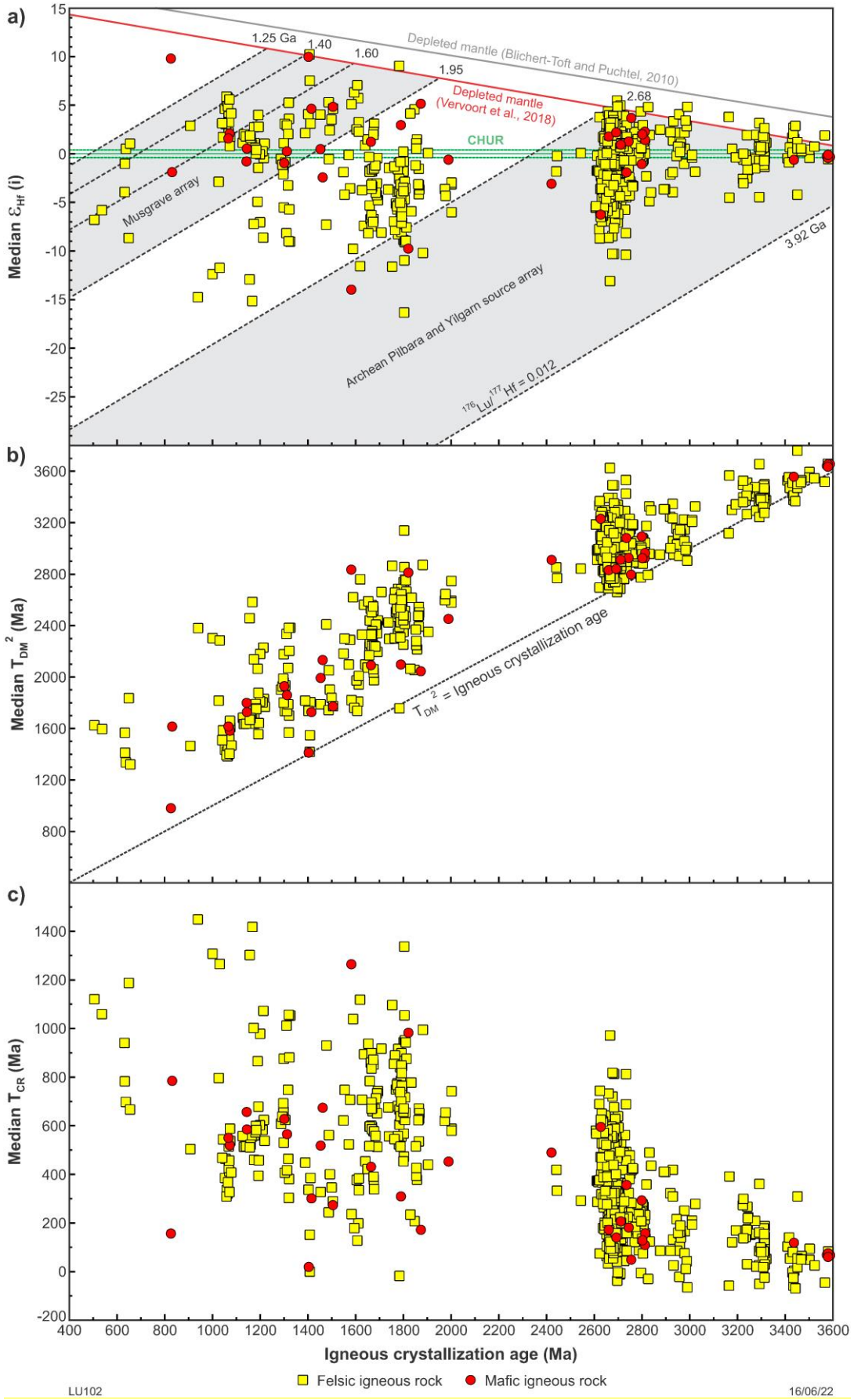

Figure 4. **Values of median $\varepsilon_{Hf(i)}$ (a), T_{DM}^2 (b), and T_{CR} (c) vs igneous crystallization age for zircon samples of felsic and mafic igneous rocks in Western Australia. Samples on or close to the depleted mantle lines in (a) or the T_{DM}^2 = igneous crystallization age line in (b) indicate juvenile mantle input. The Musgrave array and Archean Pilbara and Yilgarn source array in (a) is from Lu et al. (2022b)**

References

Belousova, EA, Kostitsyn, YA, Griffin, WL, Begg, GC, O'Reilly, SY and Pearson, NJ 2010, The growth of the continental crust: Constraints from zircon Hf-isotope data: Lithos, v. 119, p. 457–466.

Blichert-Toft, J and Puchtel, IS 2010, Depleted mantle sources through time: evidence from Lu–Hf and Sm–Nd systematics of Archean komatiites: Earth and Planetary Science Letters, v. 297, p. 598–606.

Bouvier, A, Vervoort, JD and Patchett, PJ 2008, The Lu-Hf and Sm-Nd isotopic composition of CHUR: constraints from unequilibrated chondrites and implications for the bulk composition of terrestrial planets: Earth and Planetary Science Letters, v. 273, p. 48–57.

Champion, DC and Huston, DL 2016, Radiogenic isotopes, ore deposits and metallogenic terranes: Novel approaches based on regional isotopic maps and the mineral systems concept: Ore Geology Reviews, v. 76, p. 229–256.

Fisher, CM and Vervoort, JD 2018, Using the magmatic record to constrain the growth of continental crust—The Eoarchean zircon Hf record of Greenland: Earth and Planetary Science Letters, v. 488, p. 79–91.

Griffin, WL, Wang, X, Jackson, SE, Pearson, NJ, O'Reilly, SY, Xu, X and Zhou, X 2002, Zircon chemistry and magma genesis, SE China: in-situ analysis of Hf isotopes, Pingtan and Tonglu igneous complexes: Lithos, v. 61, p. 237–269.

Hou, Z, Duan, L, Lu, Y, Zheng, Y, Zhu, D, Yang, Z, Yang, Z, Wang, B, Pei, Y, Zhao, Z and McCuaig, TC 2015, Lithospheric Architecture of the Lhasa Terrane and Its Control on Ore Deposits in the Himalayan-Tibetan Orogen: Economic Geology, v. 110, p. 1541–1575.

Kemp, AIS, Hickman, AH, Kirkland, CL and Vervoort, JD 2015, Hf isotopes in detrital and inherited zircons of the Pilbara Craton provide no evidence for Hadean continents: Precambrian Research, v. 261, p. 112–126.

Loucks, RR 2021, Deep entrapment of buoyant magmas by orogenic tectonic stress: Its role in producing continental crust, adakites, and porphyry copper deposits: Earth-Science Reviews, v. 220, p. 103744, 27p.

Lu, Y, Wingate, MTD, Champion, DC, Smithies, RH, Johnson, SP, Gessner, K, Maas, R, Mole, DR, Poujol, M, Zhao, J and Creaser, RA 2022a, Samarium–neodymium isotope map of Western Australia: Geological Survey of Western Australia, digital data layer, <www.dmirs.wa.gov.au/geoview>.

Lu, Y, Wingate, MTD, Romano, SS, Mole, DR, Kirkland, CL, Kemp, AIS, Belousova, EA, Smithies, RH, Gessner, K and Johnson, SP 2021, Zircon lutetium–hafnium isotope map of Western Australia: Geological Survey of Western Australia, digital data layer, < www.dmirs.wa.gov.au/geoview>

Lu, Y, Wingate, MTD, Smithies, RH, Gessner, K, Johnson, SP, Kemp, AIS, Kelsey, DE, Haines, PW, Martin, DM^{c}B, Martin, L and Lindsay, M 2022b, Preserved intercratonic lithosphere reveals Proterozoic assembly of Australia: Geology, doi:10.1130/G50256.1.

Lu, Y, Wingate, MTD, Smithies, RH, Johnson, SP, Martin, L, Jeon, H, Kirkland, CL, Champion, DC, Mole, DR and Gessner, K 2022c, Zircon oxygen isotope map of Western Australia: Geological Survey of Western Australia, digital data layer, <www.dmirs.wa.gov.au/geoview>.

Martin, DMcB, Murdie, RE, Kelsey, DE, Quentin de Gromard, R, Thomas, CM, Cutten, HN, Zhan, Y, Lu, Y, Haines, PW and Brett J 2022, Compilation and geological implications of the major crustal boundaries map and 3D model of Western Australia: Geological Survey of Western Australia, Record 2022/7, 49p.

Mole, DR, Fiorentini, ML, Thébaud, N, Cassidy, KF, McCuaig, TC, Kirkland, CL, Romano, SS, Doublier, MP, Belousova, EA, Barnes, SJ and Miller, J 2014, Archean komatiite volcanism controlled by the evolution of early continents: Proceedings of the National Academy of Sciences, v. 111, p. 10083–10088.

Mole, DR, Kirkland, CL, Fiorentini, ML, Barnes, SJ, Cassidy, KF, Isaac, C, Belousova, EA, Hartnady, M and Thébaud, N 2019, Time-space evolution of an Archean craton: A Hf-isotope window into continent formation: Earth-Science Reviews, v. 196, p. 102831.

Mole, DR, Thurston, PC, Marsh, JH, Stern, RA, Ayer, JA, Martin, L and Lu, Y 2021, The formation of Neoarchean continental crust in the south-east Superior Craton by two distinct geodynamic processes: Precambrian Research, v. 356, no. 106104, doi:10.1016/j.precamres.2021.106104.

Smithies, RH, Lu, Y, Gessner, K, Wingate, MTD and Champion, DC 2018, Geochemistry of Archean granitic rocks in the South West Terrane of the Yilgarn Craton: Geological Survey of Western Australia, Record 2018/10, 13p.

Söderlund, U, Patchett, PJ, Vervoort, JD and Isachsen, CE 2004, The 176Lu decay constant determined by Lu–Hf and U–Pb isotope systematics of Precambrian mafic intrusions: Earth and Planetary Science Letters, v. 219, p. 311–324.

Spencer, CJ, Kirkland, CL, Roberts, NMW, Evans, NJ and Liebmann, J 2020, Strategies towards robust interpretations of in situ zircon Lu–Hf isotope analyses: Geoscience Frontiers, v. 11, p. 843–853.

Valley, JW, Lackey, JS, Cavosie, AJ, Clechenko, CC, Spicuzza, MJ, Basei, MAS, Bindeman, IN, Ferreira, VP, Sial, AN, King, EM, Peck, WH, Sinha, AK and Wei, CS 2005, 4.4 billion years of crustal maturation: Oxygen isotope ratios of magmatic zircon: Contributions to Mineralogy and Petrology, v. 150, no. 6, p. 561–580.

Vervoort, JD and Kemp, AIS 2016, Clarifying the zircon Hf isotope record of crust–mantle evolution: Chemical Geology, v. 425, p. 65–75.

Vervoort, JD, Kemp, AI and Fisher, CM 2018, Hf isotope constraints on evolution of the depleted mantle and growth of continental crust: American Geophysical Union, Fall Meeting 2018, abstract #V23A-07.

Wang, C, Bagas, L, Lu, Y, Santosh, M, Du, B and McCuaig, TC 2016, Terrane boundary and spatio-temporal distribution of ore deposits in the Sanjiang Tethyan Orogen: insights from zircon Hf-isotopic mapping: Earth-Science Reviews, v. 156, p. 39–65.

Witt, WK, Cassidy, KF, Lu, YJ and Hagemann, SG 2020, The tectonic setting and evolution of the 2.7 Ga Kalgoorlie-Kurnalpi Rift, a world-class Archean gold province.: Mineralium Deposita, v. 55, p. 601–631.

Zhao, L, Tyler, IM, Gorczyk, W, Murdie, RE, Gessner, K, Lu, Y, Smithies, H, Li, T, Yang, J, Zhan, A, Wan, B, Sun, B and Yuan, H 2022, Seismic evidence of two cryptic sutures in Northwestern Australia: implications for the style of subduction during the Paleoproterozoic assembly of Columbia: Earth and Planetary Science Letters, v. 579, 117342.

Recommended reference

Lu, Y, Wingate, MTD, Kemp, AIS, Smithies, RH, Gessner, K, Johnson, SP, Romano, SS, Mole, DR, Kirkland, CL and Belousova, EA 2022, Zircon lutetium–hafnium isotope map of Western Australia: Geological Survey of Western Australia, digital data layer, <www.dmirs.wa.gov.au/geoview>.